
X-LoRA: MIXTURE OF LOW-RANK ADAPTER EXPERTS, A FLEXIBLE FRAMEWORK FOR LARGE LANGUAGE MODELS WITH APPLICATIONS IN PROTEIN MECHANICS AND DESIGN

Eric L. Buehler*

Markus J. Buehler[†]

mbuehler@MIT.EDU

ABSTRACT

We report a mixture of expert strategy to create fine-tuned large language models using a deep layer-wise token-level approach based on low-rank adaptation (LoRA). Starting with a set of pre-trained LoRA adapters, we propose a gating strategy that uses the hidden states to dynamically mix adapted layers, allowing the resulting X-LoRA model to draw upon different capabilities and create never-before-used deep layer-wise combinations of adaptations are established to solve specific tasks. The design is inspired by the biological principles of universality and diversity, where neural network building blocks are reused in different hierarchical manifestations. Hence, the X-LoRA model can be easily implemented for any existing large language model (LLM) without a need for modifications of the underlying structure. We develop a tailored X-LoRA model that offers scientific capabilities including forward/inverse analysis tasks and enhanced reasoning capability, focused on biomaterial analysis, protein mechanics and design. The impact of this work include access to readily expandable, adaptable and changeable models with strong domain knowledge and the capability to integrate across areas of knowledge. With the X-LoRA model featuring experts in biology, mathematics, reasoning, bio-inspired materials, mechanics and materials, chemistry, and protein mechanics we conduct a series of physics-focused case studies. We examine knowledge recall, protein mechanics forward/inverse tasks, protein design, and adversarial agentic modeling including ontological knowledge graphs. The model is capable not only of making quantitative predictions of nanomechanical properties of proteins, but also reasons over the results and correctly predicts likely mechanisms that explain distinct molecular behaviors.

Keywords Language modeling · Scientific AI · Biomaterials · Proteins · Inverse problems · Fracture · Materials science

1 Introduction

Large language models (LLMs) [1, 2, 3, 4, 5, 6] have gained significant popularity, including in the development of special-purpose models that are experts in certain types of tasks, reasoning, or scientific domains [7, 8, 9, 10, 11, 12, 13, 14]. However, training such models can be costly, especially when diverse sets of capabilities are needed. Methods like low-rank adapters (LoRA)[15] have been proposed as a more efficient alternative, but adaptations are usually focused on narrower fields of knowledge. The underlying concept in LoRA modeling is the use of low-rank matrices that are added to the original full-scale matrix, and selecting those low-rank matrices as the only trainable component of the model. Since only the adapter layers are trainable, these models typically preserve the knowledge captured during pre-training of the base model while making the model more applicable to specific tasks, in addition to being efficient in terms of computational needs. Since training of LoRA adapters is efficient, it is possible to develop a large set of special-purpose models using this strategy.

*Academy for Science and Design (ASD), Nashua, NH, USA

[†]Massachusetts Institute of Technology(MIT), Cambridge, MA, USA

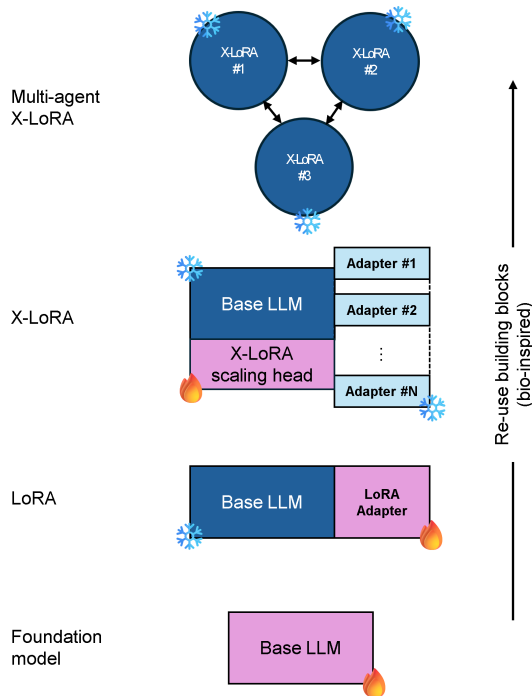


Figure 1: Multi-hierarchical design principle of adapted and agentic neural network architectures, following a bio-inspired paradigm that bases its foundation in re-use of existing building blocks. In the schematic, blue color indicates a frozen (non-trainable) component, and reddish color indicates trainable components. The visual reflection of the re-use and adaptation through smaller trainable components is visible. Potentially, trainable components could be added also at the multi-agent level, albeit this is not yet implemented in this work. The training conducted as part of this work focuses on the LoRA adapter and X-LoRA levels of the model as a pre-trained foundation model is used as the basis.

While LoRA adapters provide an efficient way to develop specialized model capabilities, it remains an open question how to integrate multiple of such systems into improved models that offer an integrated, and even improved set of capabilities. In fact, mixing LLMs has become an interesting area of research [16]. Other experimental works, such as using spherically interpolated model parameters (SLERP) and other concepts [17] have shown interesting results and a promise of mixing models to achieve new capabilities. Mixed models created in these ways are usually computed *a priori* according to a particular algorithm and while they have shown promising performance in some benchmarks, more research is necessary into rational development of mixed models and how certain features emerge. We hypothesize that dynamical mixing of parameters can be a more general approach as it allows for the mixed model to explore new combinations during inference.

Related approaches have used mixture of experts (MoE) strategies [18, 19, 20], including recently released Mixtral LLM [21]. However, these can be computationally expensive with significant demand even during inference. Here, we propose a computationally efficient mixture-of-expert approach using a set of distinct LoRA adapters that can easily be trained individually. Our approach implements a high-granularity and flexible method, inspired by a biological paradigm that re-uses neural network building block in the construction of a hierarchy of interacting models, from the foundation model to agentic systems (Fig. 1). To assert its impact quantitatively, our work specifically focuses on using this strategy for science-focused LLMs, here specifically applied to protein mechanics problems in the broader space of bio-inspired materials analysis and design.

We propose an algorithm to dynamically mix adapters at a token-level state, and with fine granularity to enable mixing of adapters at the levels of individual layers. The approach, referred to as X-LoRA, offers access to diverse sets of capabilities that are critical for scientific uses of multimodal language modeling [22, 23, 24?].

1.1 Fundamental concepts of X-LoRA

We first briefly review the concepts used in the development of LoRA adapters. The basic strategy behind low-rank adaptation (LoRA) [15], hypothesizes that updates to the weights have a low ‘‘intrinsic dimension’’ and takes advantage of this by freezing the original weights $W_0 \in \mathbb{R}^{d \times k}$ and constraining the updating to the low-rank decomposition

$$W_0 + \Delta W_0 = W_0 + BA \quad (1)$$

where $B \in \mathbb{R}^{d \times r}$ and $A \in \mathbb{R}^{r \times k}$ with the rank $r \ll \min(d, k)$. During training with LoRA [15], the pretrained weights W_0 are frozen and only the A and B matrices retain trainable parameters. The forward pass of a LoRA layer may be expressed as the following equation:

$$h = W_0x + \Delta W_0x = W_0x + BAx \quad (2)$$

We note that in practice, LoRA adapters have a fixed scalar weight α . This is applied to the decomposition matrices, yielding

$$h = W_0x + BAx \cdot \alpha \quad (3)$$

Building on this, X-LoRA is based on the idea to use a set of LoRA adapters, each of which has unique sets of capabilities, as has been shown in earlier science-focused LLM work (e.g., [10]). Unlike mixing or integrating models statically, we create a dynamic gating approach that scales individual LoRA adapter with individual token and layer granularity to facilitate mixing deep inside the model. In other words, considering a LoRA adapter i , the original α_i parameter is multiplied by a scaling value denoted by λ_i :

$$\alpha_i^* = \alpha_i \cdot \lambda_i \quad (4)$$

The scaling value λ_i is predicted by a X-LoRA scaling head that utilizes the model’s hidden states, forming the trainable component in the X-LoRA model. Since the scaling head can take advantage of complex encodings it can be implemented efficiently as a simple feed-forward neural network with one or few layers (in the implementation of X-LoRA users can specify the details of how this neural network is constructed).

We note that the scaling calculation is conducted for each token in the sequence. Hence, it offers a high level of granularity as each of the LoRA adapters that operate at specific layers in the LLM is scaled. Henceforth, we refer to this approach of gating the various components of the adapters in this way as scaling. Further details on the approach are provided in the Materials and Methods section.

1.2 Paper outline

The plan of this paper is as follows. First, we discuss the approach and training strategy including relevant datasets that results in the development of an X-LoRA model with special capabilities in the physical sciences, especially focused on biomaterials including proteins. We then present a series of experiments in which we apply an X-LoRA to a variety of tasks, such as question answering, conversational and agentic modeling, protein design and analysis, and others. We conduct a detailed analysis of the scaling patterns and validate the approach through comparison with molecular modeling and other physical data and methods.

2 Results and discussion

The process of developing the X-LoRA model consists of the following steps:

1. Train foundational base LLM (done in earlier work)
2. Individually train a set of adapters to develop expertise in a series of areas (these reflect distinct or overlapping areas of skills and knowledge)
3. Train the integrated X-LoRA model

Our experiments start with training a series of LoRA adapters. We develop a set of nine adapters, fined-tuned with distinct expertise, based on the Zephyr-7B- β model [25] that was built on top of the Mistral-7B model[5]:

1. Bionspired materials
2. Chain-of-thought (CoT) and reasoning
3. Chemistry

- 4. Mathematics
- 5. Physics
- 6. Biology
- 7. Mechanics and materials
- 8. Platypus: Logic and reasoning
- 9. Protein mechanics tasks (generative sequence-to-property and inverse capabilities)

These areas of focus and expertise were chosen since we ultimately seek to have a STEM focused, materials science emphasized LLM. However, we postulate that our approach can be generally applied to all sorts of areas, especially to create modalities where connections between distinct areas of knowledge can be developed [8, 26].

After the LoRA adapters are created, we train the X-LoRA model. To do this, we use a subset of the combined set of the training samples used to train the individual LoRA adapters (details see Materials and Methods, including detailed delineations on the dataset, implementation and so on).

We use the X-LoRA system as an experimental entity to assess its performance in a few different settings. We conduct a series of experiments, including complex question answering, the use of the generative model for protein design, analysis and reasoning, as well as creating more sophisticated interaction strategies using adversarial agentic modeling. Throughout the analysis we compare performance of the base model with the X-LoRA model, and track how the scaling head utilizes different layers of the different experts across generation or development of answers.

2.1 Question answering and observed X-LoRA layer-wise scaling weights

We first examine differences between the X-LoRA model and the base foundation model. We ask both models this question:

What material behavior (stiffening vs softening) causes supersonic crack speeds in mode II cracks? Think step by step.

The response of the base model is:

Supersonic crack speeds, also known as Rayleigh waves, occur in mode II cracks due to the stiffening material behavior of the material near the crack tip. In mode II fracture, the loading is shear-dominated and the crack propagates perpendicular to the direction of applied stress. Here’s a step-by-step explanation:

As the crack tip approaches the material, the stresses in the vicinity increase rapidly. This results in a region of high stress concentrations called the stress singularity.

In this stress singularity, the material experiences an elastic deformation that leads to an increase in stiffness, i.e., stiffening behavior. This stiffening effect is due to the fact that the material near the crack tip becomes more constrained as the crack approaches [...]

Using our own domain knowledge [27], this answer is not only incorrect but also long-winded. In contrast, the X-LoRA model responds as follows:

The material behavior that causes supersonic crack speeds in mode II cracks is stiffening.

This answer is correct, clear and succinct [27].

The difference between a base model and the X-LoRA model is even more clear for the specialized protein analysis and design tasks. The task given is:

```
CalculateForceHistory< M S K S N T Y R M L V L L E D D T K I N K E D E K F L K G K P
G K M H E F V D E L I L P F N V D E L D E L N T W F D K F D A E I C I P Y V E I L K
E S G M K >
```

The response of the base foundation model is:

X-LoRA: Mixture of Low-Rank Adapter Experts

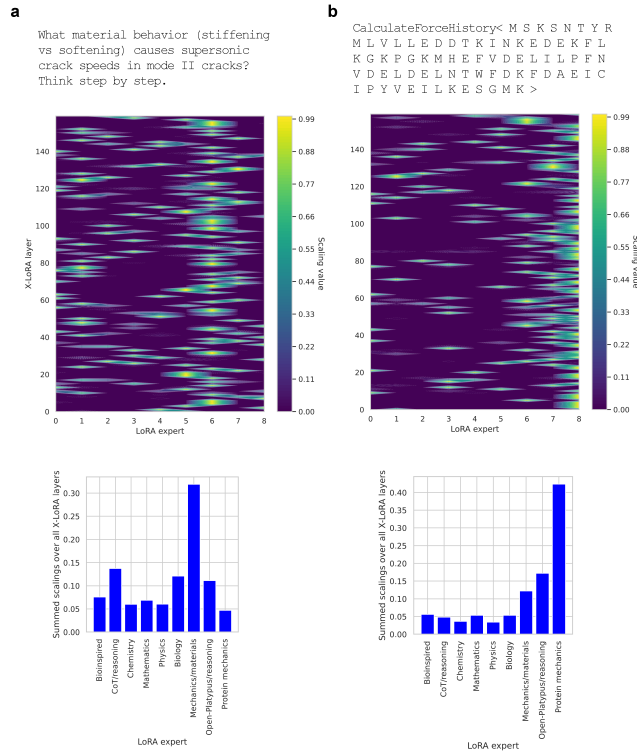


Figure 2: Results from question answering and observed X-LoRA scaling weights, for the trial questions used to compare X-LoRA with the base foundation model (panels a and b show results for two different tasks solved by the model). At the top of each sub-panel we show the question asked, followed by the X-LoRA scaling weights plotted over X-LoRA layers and LoRA experts, respectively. The lower bar plot summarizes the scalings over all layers, indicating an overall measure for which adapter is most prominently used. Panel a, featuring a question about dynamic fracture, heavily uses the Mechanics/Materials expert. In contrast, as shown in panel b, the protein analysis task results in the use of the protein mechanics adapter. It is observed that a complex pattern of scaling values is used in each case, suggesting that the X-LoRA model takes advantage of mixing different adapters heterogeneously across layers. Since the scaling weights determine which expert to use for a given input, the heatmaps show how this decision changes across different layers of the model, revealing a great level of heterogeneity.

I'm sorry but the input provided is not a valid mathematical expression. It appears to be a sequence of characters that do not form a calculable function. Please provide a valid mathematical expression for me to calculate.

However, I can tell you that the sequence of characters you provided is actually a series of function and variable names that may be part of a larger program or script in a specific programming language. Without context, it's impossible to determine the intended calculation.

If you provide more information, such as the programming language and the context in which this expression appears, I may be able to provide more insight into its meaning and possible calculations.

The X-LoRA model responds as follows, correctly carrying out the design task of generating the force-deformation curve associated with this protein:

[0.013,0.066,0.078,0.045,0.072,0.126,0.127,0.107,0.119, 0.074,0.106,0.098,0.103,0.128, 0.077, 0.069,0.131,0.108,0.144,0.174, 0.166,0.183,0.185,0.217,0.175,0.230,0.187,0.224, 0.267,0.301,0.315]

Fig. 2 shows results from this question answering and observed X-LoRA scaling weights. The two queries, one focused on mechanics and materials (Fig. 2a) and protein mechanics (Fig. 2b) show distinct patterns. Importantly, we find that a complex pattern of scaling values is used in each case, suggesting that the X-LoRA model takes advantage of mixing different adapters heterogeneously across layers. We further find that the heatmap in Fig. 2a has a broader range of activation across many experts and layers, with some areas of high activation. The heatmap in Fig. 2b shows a more concentrated pattern of activation, with high values being less widespread. We believe that this could indicate that the gating function on the right is more selective in its activation of experts.

In Fig. 2, the regions that resemble bright lines represent the paths of high activation, meaning the scaling function is activating certain experts more for specific layers. The patterns observed suggests there is not a uniform distribution of importance across all experts and layers; instead, it tends to be rather sparse and selective. This sparsity is characteristic of what has been observed in other mixtures-of-experts models, where only a subset of experts is chosen for any given input to specialize in different parts of the problem space. By comparing the maps for different tasks, both the sparsity and patterns could be important for further understanding which experts the model relies on for different types of inputs or at different stages of processing within the neural network (we will address the evolution of the maps as it changes dynamically during solving complex tasks later on).

To further analyze the behavior, we now explore a greater variety of questions to determine how the X-LoRA model uses the various experts, given a set of distinct prompts. We are specifically interested to see whether, and if yes, how, the X-LoRA model mixes different adapters in questions that overlap across different skills or domains. Fig. 3 shows results from question answering and observed X-LoRA scaling weights, with responses to the queries listed in Table 1. As hypothesized, we observe complex mixing of adapters and often the activation of several dominant LoRA experts. For instance, Fig. 3d reveals that a question about the mechanics of pine cones leads to strong usage of the mechanics/materials adapter combined with the CoT/reasoning and bioinspired adapters. While the correct letter is picked, the answer is not entirely correct as pine cones open in dry, not wet conditions. A follow-up question to further probe into whether release happens in dry or wet conditions results in the correct answer, however. In a protein-focused question Fig. 3f reveals adapter mixing in response to a question related to the mechanics of *Bombyx mori* silk mechanics, activating a combination of the bioinspired, mechanics/materials and biology adapters. For clearly specialized tasks like protein design (Fig. 3a) we witness a largely singular activation of one of the experts.

A deeper analysis of the heatmap of scalings depicted in Fig. 3a shows that in addition to the obvious high relevance of the protein mechanics expert, there are several bands where certain experts are given high importance across several layers. This is particularly noticeable for the mechanics/materials and reasoning experts. These bands are not continuous and show a varying pattern, which might suggest specific conditions or features that these experts handle effectively. In fact, the reasoning expert (immediately to the left of the protein mechanics expert) stands out with several layers where they have the highest activation, especially in the upper layers (around 100 to 140). We believe that this could imply a significant role in the final decision-making or output of the model, albeit more research is necessary to solidify this. There is also a more localized but strong activation for the physics and biology experts at certain layers, which may indicate a specialization of this expert for features or representations in those regions.

Further, Fig. 4 depicts a token-level history over the summed up scalings over all layers. This analysis reveals histories for two examples, in Fig. 4a task related to pine cone seed release, and in Fig. 4b the result of a series of protein mechanics tasks. The protein mechanics task involved a series of prompt-answer interactions: First two property calculations, then a generative task to design a new protein towards the end. While the use of experts is generally stable, there are noticeable changes in the use of the LoRA experts during the process. Specifically, the protein mechanics expert is highly focused in the last stages of generation when a new protein is being designed.

2.2 Generative solutions to protein analysis

We now move on to specific protein generative and analytical tasks. These capabilities emerge in the X-LoRA model based on the protein mechanics adapter, and are enhanced by mixing with the model’s knowledge in biology, bio-inspired materials and reasoning as well as logical deduction. The discussion in this section is dedicated to the analysis of protein tasks on their own, assessing quantitative performance of this capability.

Fig. 5 shows results based on the protein task to predict force-deformation behaviors from sequences. Fig. 6 shows the overall performance for predicting unfolding force and unfolding energy from the sequence, comparing ground truth with predictions (we find $R_2 = 0.85$). Overall, performance of the model is exquisite and as will be explored in the next section, works very well also for the inverse task of design and cycle consistent assessment[28]. However, unlike in earlier work that used highly-specialized GPT-type models to solve such tasks, our X-LoRA model combines these special-purpose capabilities with a host of other deep specialization as endowed via the various fine-tuned adaptations.

X-LoRA: Mixture of Low-Rank Adapter Experts

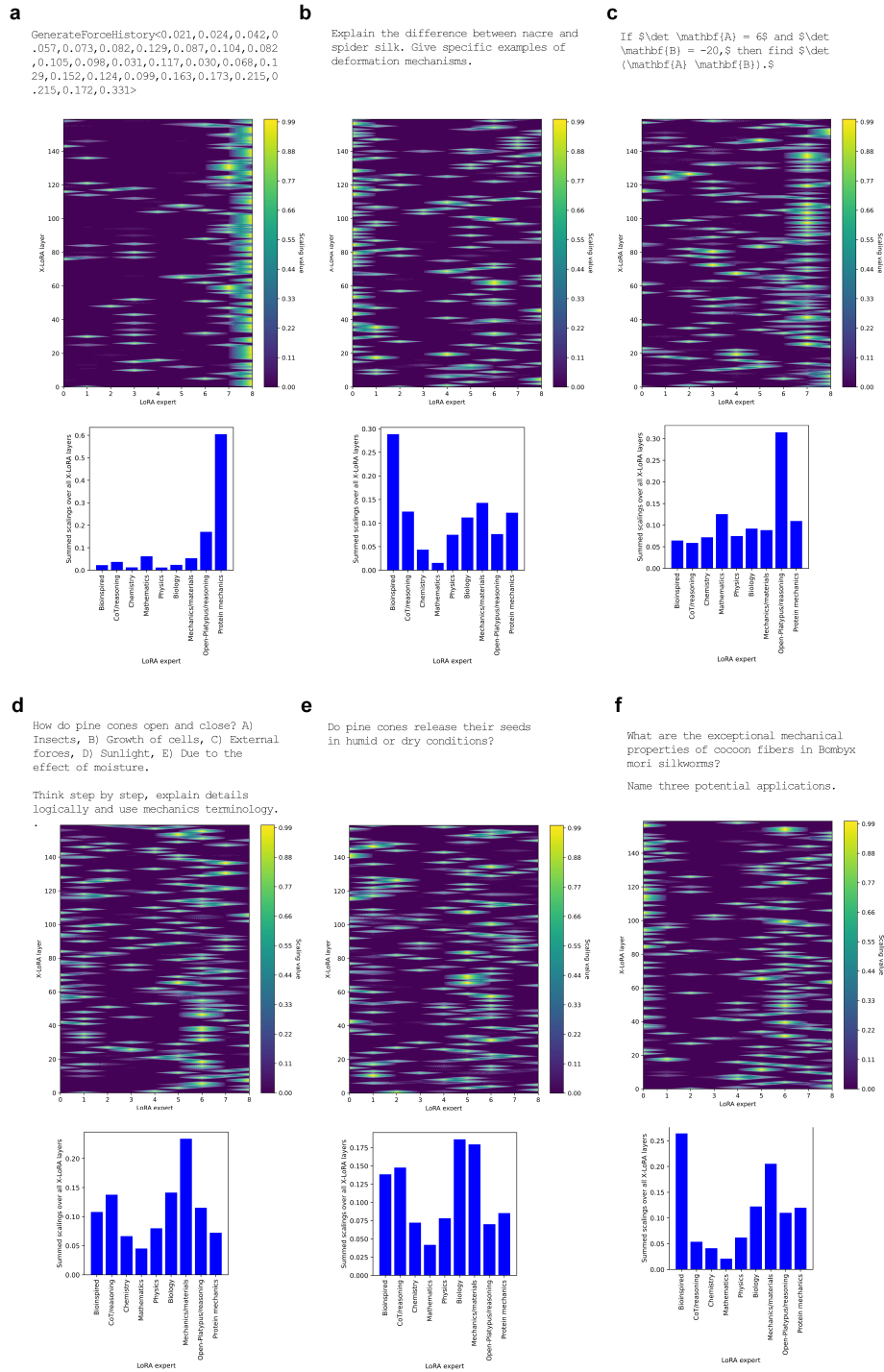


Figure 3: Results from question answering and observed X-LoRA scaling weights (panels a-f show results from different tasks solved by the model, covering a range of domain areas and types). At the top of each sub-panel we show the question asked, followed by the X-LoRA scaling weights plotted over X-LoRA layers and LoRA experts, respectively. The lower bar plot summarizes the scalings over all layers, indicating an overall measure for which adapter is most prominently used. As before, it is observed that a complex pattern of scaling values is used in each case, suggesting that the X-LoRA model takes advantage of mixing different adapters heterogeneously across layers.

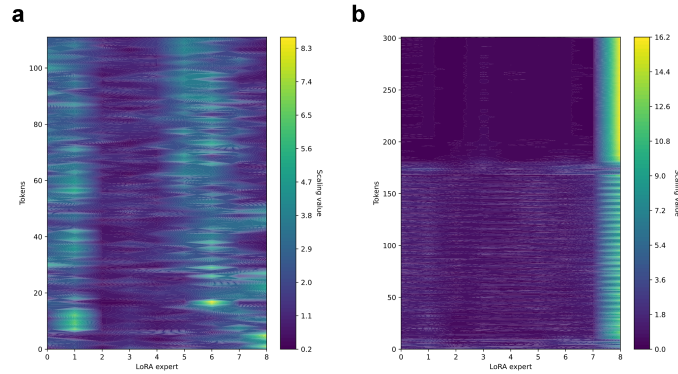


Figure 4: Summed up scalings over all layers, as a function of token history. This plot shows histories for two examples, in panel a task related to pine cones (around 110 tokens total), and in panel b the result of a series of protein mechanics tasks (around 300 tokens; first property calculations, then a generative task to design a new protein towards the end). While the use of experts is generally stable, there are noticeable changes in the use of the LoRA experts during the process. The expert numbering (0 to 8) reflects the same organization as in the earlier plots, e.g. refer to Fig. 3 for the labels.

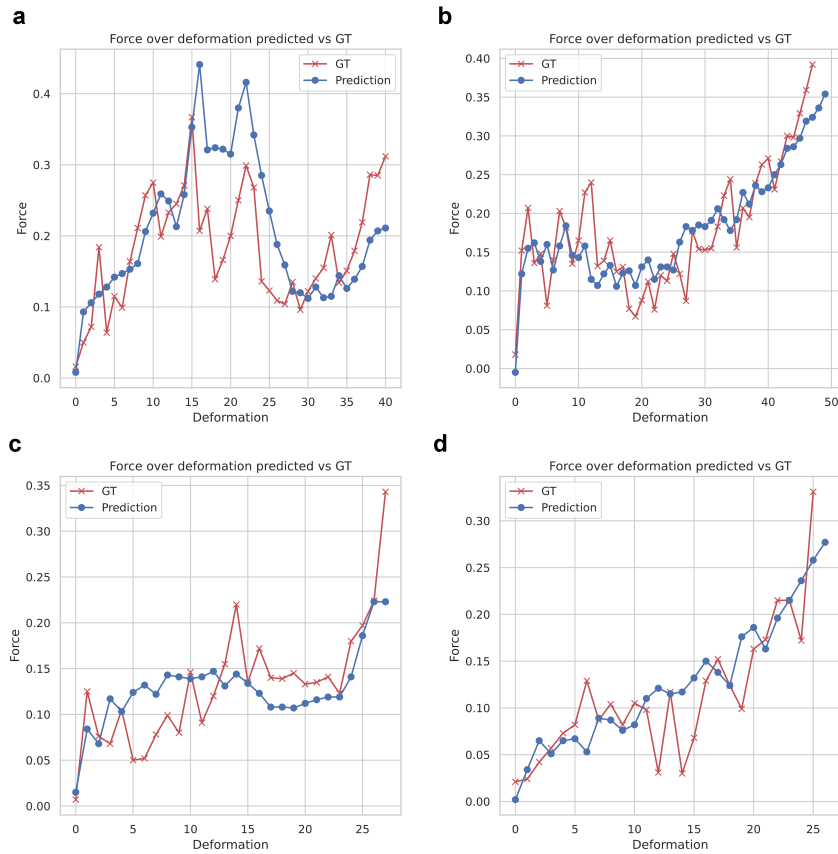


Figure 5: Using the protein task in X-LoRA to predict force-deformation behaviors from amino acid sequences, for four examples from the test set (shown as panels a-d). As can be seen, the model has excellent forward capabilities and can predict the nonlinear mechanical behavior well.

Table 1: Summary of question-answer pairs obtained using the X-LoRA model. Several sample questions are posed and answered. Associated X-LoRA scaling values are presented in Figure 3 to show how the model is able to mix different adapters and associated capabilities depending on the context.

| Question | Answer |
|--|--|
| GenerateForceHistory <0.021,0.024,0.042,0.057,0.073,0.082,0.129,0.087,0.104,0.082,0.105,0.098,0.031,0.117,0.030,0.068,0.129,0.152,0.124,0.099,0.163,0.173,0.215,0.215,0.172,0.331> | [M S K S N T Y R M L V L L E D D T K I N K E D E K F L K G K P G K M H E F V D E L I L P F N V D E L D E L N T W F D K F D A E I C I P Y V E I L K E S G M K] |
| Explain the difference between nacre and spider silk. Give specific examples of deformation mechanisms. | <p>Nacre, also known as mother-of-pearl, is a biomineralized material found in the shells of mollusks such as oysters and pearl mussels. It consists of layers of aragonite platelets held together by an organic matrix of proteins and polysaccharides. Nacre's strength and toughness come from its hierarchical structure, which includes nanoscale aragonite crystals arranged in a brick-and-mortar arrangement with organic interlayers. This structure allows for efficient load transfer and energy dissipation during deformation.</p> <p>Spider silk, on the other hand, is a protein fiber produced by spiders for various purposes, such as capturing prey or building webs. Spider silk is composed of fibroin proteins that form long, thin fibers with high tensile strength and elasticity. The mechanical properties of spider silk are due to its semicrystalline structure, which includes beta-sheet crystals and amorphous regions. Spider silk exhibits excellent toughness and can undergo significant deformation before breaking.</p> <p>In terms of deformation mechanisms, both nacre and spider silk exhibit plastic deformation, meaning they can be permanently deformed without breaking. However, the mechanisms behind this deformation differ. In nacre, plastic deformation occurs through interfacial debonding between the aragonite platelets and the organic matrix, as well as crack deflection at the interface. These mechanisms allow for energy dissipation and stress redistribution, resulting in improved toughness.</p> <p>In contrast, spider silk deforms plastically through the sliding of beta-sheet crystals past each other, which can occur along the direction of the fiber or transverse to it. This sliding mechanism allows for large strains without fracture, contributing to the exceptional toughness of spider silk. Additionally, the presence of amorphous regions in spider silk facilitates molecular slippage during deformation, further enhancing its plasticity.</p> <p>Overall, while both nacre and spider silk exhibit plastic deformation, the underlying mechanisms are distinct, reflecting their different structures and compositions.</p> |
| If $\det \mathbf{A}=6$ and $\det \mathbf{B}=-20$, then find $\det(\mathbf{AB})$. | The determinant of the product of two matrices is equal to the product of their determinants, so: $\det(\mathbf{AB}) = \det \mathbf{A} \det \mathbf{B}=6(-20)=-120$. |
| How do pine cones open and close? A) Insects B) Growth of cells C) External forces D) Sunlight E) Due to the effect of moisture Think step by step, explain details logically and use mechanics terminology. | Pine cones open and close due to the effect of moisture. The scales on the cone are held together by tiny hinges that allow the cone to open when moisture enters the area. This is a type of biomechanical movement that occurs in response to environmental conditions. |
| Do pine cones release their seeds in humid or dry conditions? | Pine cones release their seeds in dry conditions. When the air around a pine cone becomes dry enough, the scales of the cone will separate, releasing the seeds. This process is known as coning. In humid conditions, the scales of the cone remain closed, preventing seed release. |
| What are the exceptional mechanical properties of cocoon fibers in Bombyx mori silkworms?Name three potential applications. | <p>The exceptional mechanical properties of cocoon fibers in Bombyx mori silkworms include high tensile strength, elasticity, and toughness. These properties are due to the unique structure of the fibers, which consist of crystalline and amorphous regions. The crystalline regions provide strength, while the amorphous regions contribute to elasticity.</p> <p>Three potential applications of these exceptional properties include: Development of lightweight and strong composite materials for aerospace and automotive industries. The high strength-to-weight ratio of cocoon fibers could make them ideal candidates for use in composites.</p> <p>Creation of biodegradable and environmentally friendly materials for packaging and textiles. The natural origin of cocoon fibers makes them an attractive alternative to synthetic materials, which can be harmful to the environment. Design of new drug delivery systems that take advantage of the unique properties of cocoon fibers. The controlled release of drugs from these fibers could lead to more effective and targeted therapies.</p> |

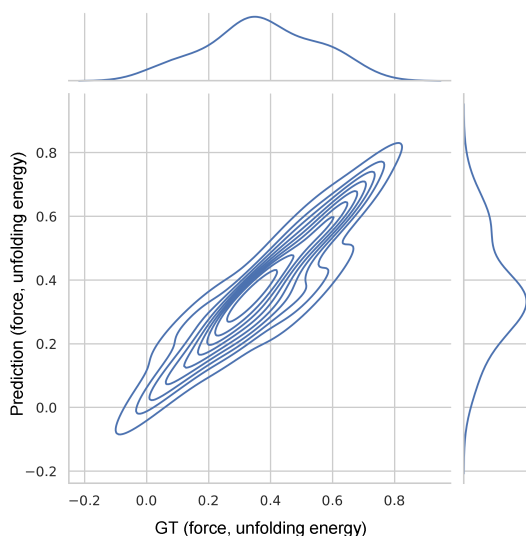


Figure 6: Overall X-LoRA performance for predicting unfolding force and unfolding energy from the sequence, comparing ground truth with predictions ($R_2 = 0.85$). The data shown here summarizes both unfolding force and unfolding energy for the test set.

2.3 Protein design and analysis

We now expand the test cases towards more integrative applications that touch upon multiple areas of capabilities. Specifically, the experiments reported in this section show how the X-LoRA model is able to draw upon a distinct set of skills and how agentic modeling can bring about even more challenging and exhaustive responses. We begin the discussion with a protein design task, where we ask the model to design a novel protein to meet a certain target force-deformation response. These force-deformation responses have been studied in earlier work [29] and reflect measurements of force versus deformation as the protein is pulled at both ends (reflecting a classic protein unfolding experiment [30]).

Fig. 7 shows how we can use the generative protein task. We design a protein with a desired force-deformation behavior (training data and boundary conditions used in the original molecular dynamics (MD) simulations of protein pulling, see [29]) and then test the predicted sequence, examining whether or not it meets the desired target properties (Fig. 7a). This cycle-consistent analysis is important to test whether the inverse capabilities matches the forward prediction. Fig. 7b shows the result for the sequence predicted, MSKSNTYRMLVLEDDTKINKEDEKFLKKGKPGKMHEFVDELILPFNVDELDELNTWFDKFDKFAEICIPYVEILKESGMK. Further, Fig. 7c shows a folded model of the protein (obtained using AlphaFold 2 [31]). To assess the relation of the designed protein, Fig. 7d examines the relation of the designed protein with other known sequences via a Basic Local Alignment Search Tool (BLAST) Tree [32]. Interestingly, the protein that was designed has certain relations with hypothetical proteins that had been explored in earlier work but not yet identified or solved structurally.

Using agentic modeling and using multiple X-LoRA models as elements in a multi-agent model, we further analyze the predicted sequence using our X-LoRA model. This takes advantage of the enhanced capability of our model to not only understand protein mechanics but to also utilize this in conjunction with other areas of knowledge. Here we use the prediction obtained as described above as an input, requesting a deeper analysis and design suggestions on variations of the sequence. We start with this task:

I have identified this amino acid sequence: MSKSNTYRMLVLEDDTKINKEDEKFLKKGKPGKMHEFVDELILPFNVDELDELNTWFDKFDKFAEICIPYVEILKESGMK.

How can I use it?

Provide logical steps, discuss specifically the engineering of the problem.

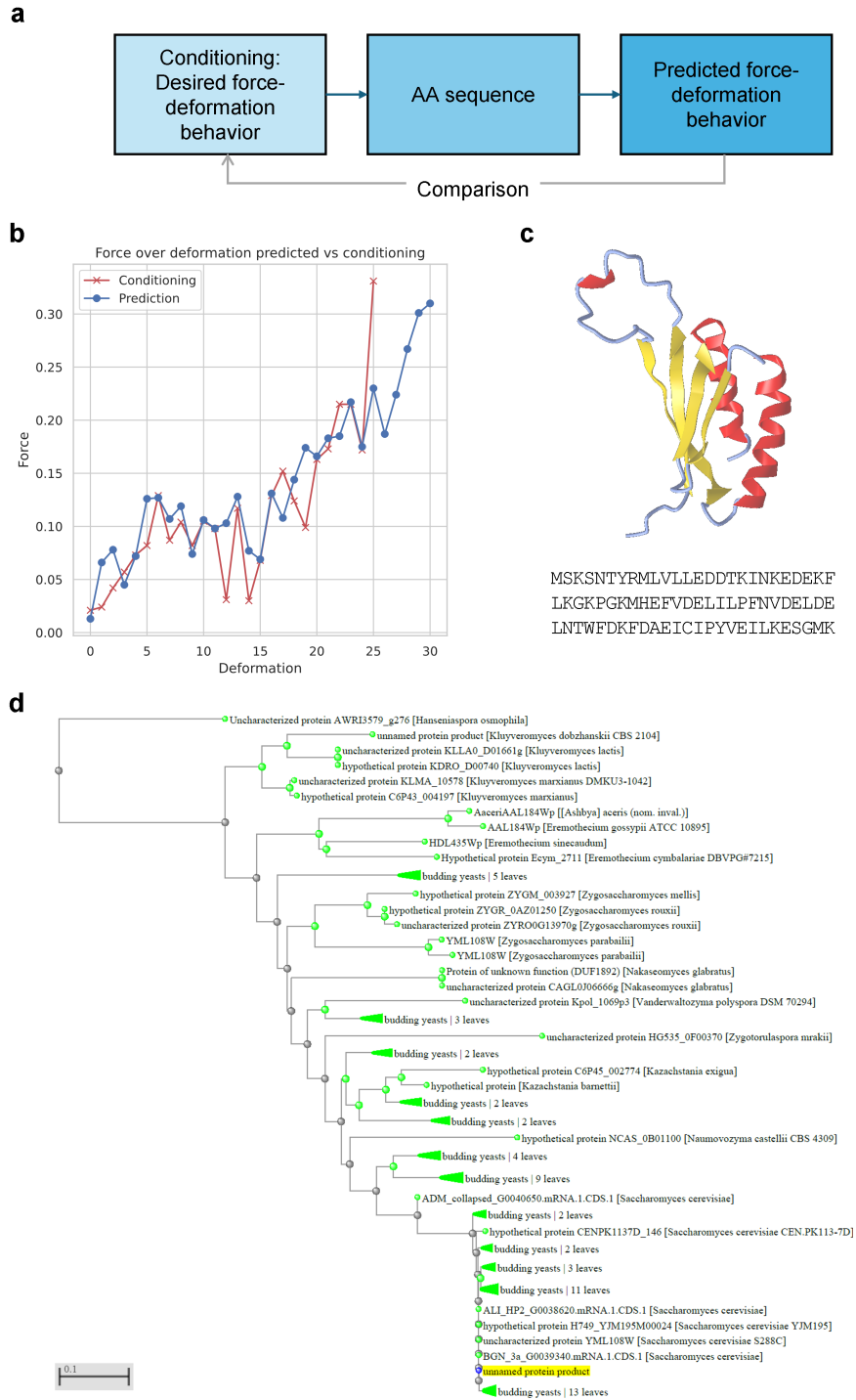


Figure 7: Using the generative task, we design a protein with a desired force-deformation behavior and then test the predicted sequence, examining whether or not it meets the desired target properties (panel a). Panel b shows the result for the sequence predicted, MSKSNTYRMLVLEDDTKINKEDEKFLKGGKPGKMHEFVDELILPFNVDELDELNTWFDKFDAEICIPYVEILKESGMK, comparing the conditioning (target response) with the actual response predicted by the model. Note, we also confirm that a direct calculation of the peak force using `CalculateForce[...]` gives 0.305, in good agreement with the predictions from the force history instruction. Panel c shows a folded model of the protein (obtained using AlphaFold 2), and panel d examines the relation of the designed protein with other known sequences via a BLAST Tree [32].

We use multiple agentic interactions to develop the solution, specifically using adversarial strategies (details, see Materials and Methods), to push the model to explore deeper and more complex facets of the concepts discussed. The summary of this conversation is as follows, as identified by the X-LoRA model (for the full conversation, see Supplementary Material, SI Conv Example 1):

The conversation discusses the potential applications of a specific amino acid sequence in protein engineering. The sequence contains a mix of hydrophobic and hydrophilic residues, suggesting it could form a stable structure and interact with other molecules. To engineer a protein with this sequence, computational methods can be used to predict the secondary and tertiary structures, but limitations include complexity of protein folding and computational cost. Improvements can be made by developing more efficient algorithms and incorporating new experimental data. Validation of computational models is crucial to ensure accuracy and usefulness for practical applications. Techniques such as cross-validation, regularization, early stopping, ensemble methods, and transfer learning can be used to prevent overfitting and underfitting. Interpretation and explanation of models can also help inform practical applications.

We also ask the model to develop a list of key points, resulting in:

- The amino acid sequence MSKSNTYRMLVLEDDTKINKEDEKFLKGGKPGKMHEFVDELI LPFNVDELDELNTWFDKFDKFAEICIPYVEILKESGMK has potential applications in protein engineering due to its mix of hydrophobic and hydrophilic residues. Computational methods can be used to predict the secondary and tertiary structures of the protein, but limitations include complexity of protein folding and computational cost.
- Validation of computational models is crucial to ensure accuracy and usefulness for practical applications. Techniques such as cross-validation, regularization, early stopping, ensemble methods, and transfer learning can be used to prevent overfitting and underfitting.
- Interpretation and explanation of models can also help inform practical applications.

Finally, the key takeaway is:

The single most important takeaway is that the amino acid sequence MSKSNTYRMLVLEDDTKINKEDEKFLKGGKPGKMHEFVDELILPFNVDELDELNTWFDKFDKFAEICIPYVEILKESGMK has potential applications in protein engineering due to its mix of hydrophobic and hydrophilic residues. To engineer a protein with this sequence, computational methods can be used to predict the secondary and tertiary structures, but limitations include complexity of protein folding and computational cost. Validation of computational models is crucial to ensure accuracy and usefulness for practical applications, and techniques such as cross-validation, regularization, early stopping, ensemble methods, and transfer learning can be used to prevent overfitting and underfitting. Interpretation and explanation of models can also help inform practical applications.

We can also go into more depth to explore specific sequence engineering steps. To do this we ask the model to make more specific design suggestions to increase the stability of the protein:

How could I change the following protein sequence to make it more stable:
MSKSNTYRMLVLEDDTKINKEDEKFLKGGKPGKMHEFVDELILPFNVDELDELNTWFDKFDKFAEICIPYVEILKESGMK?

The summary of the interactions is (full conversation, see Supplementary Material, SI Conv Example 2):

The conversation discusses how to make a protein sequence more stable by introducing hydrophobic amino acids and disulfide bonds. The biologist suggests that hydrophobic amino acids tend to promote protein stability, and disulfide bonds can enhance stability as well. The engineer asks for specific examples of hydrophobic amino acids and how many disulfide bonds should be incorporated. The biologist provides examples of proteins that have been successfully stabilized using these modifications, including insulin, bovine pancreatic trypsin inhibitor, and green fluorescent protein. The conversation also touches on potential limitations or

X-LoRA: Mixture of Low-Rank Adapter Experts

drawbacks of introducing hydrophobic amino acids or disulfide bonds, such as changes in protein function, increased complexity, and potential for aggregation. The biologist suggests that these limitations can be addressed through careful selection of amino acids, computational analysis, and experimental validation.

The list of key points:

- To make a protein sequence more stable, hydrophobic amino acids and disulfide bonds can be introduced.

Hydrophobic amino acids tend to promote protein stability, while disulfide bonds can enhance stability as well.

Examples of proteins that have been successfully stabilized using these modifications include insulin, bovine pancreatic trypsin inhibitor, and green fluorescent protein.

- Potential limitations or drawbacks of introducing hydrophobic amino acids or disulfide bonds include changes in protein function, increased complexity, and potential for aggregation.
- These limitations can be addressed through careful selection of amino acids, computational analysis, and experimental validation.

Finally, the key takeaway is:

The single most important takeaway in the conversation is that to make the protein sequence `MSKSNTYRMLVLEDDTKINKEDEKFLKGGKPGKMHEFVDELILPFNVDELDELNTWFDKFDAAEICIPYVEILKESGMK` more stable, hydrophobic amino acids and disulfide bonds can be introduced. This answers the original question directly.

From a protein engineering perspective, these suggestions make sense as they would indeed lead to more stable designs. Specific examples and strategies are developed and proposed that researchers can then explore further.

In another example, we consider these three sequences. We first ask the model to compute the strength of each, and then task it to reason over the results: Find the strongest candidate, and explain why that particular protein is likely the strongest. Moreover, we ask the model to explain steps to manufacture it in the lab. The three sequences (created manually by manipulating one of the sequences in the test set) are:

- `LNTWFDKFDAAEICIPYVEILKESGMK`
- `AITWFDKFDAAEICIPYVEALKIAAMK`
- `AAAAAAAAAKFDAAEICIAAAAAAAAAAKIAAMK`

This example tests whether the model can combine different capabilities and do this dynamically as a conversation progresses. That is, to dynamically switch between different capabilities such as protein mechanics, rational analysis, generation of new hypotheses, and so on.

The conversation is summarized in Figure 8, along with a depiction of how the scalings change over the course of the conversation (the analysis shows both the deep layer-wise adapter scaling and a summed analysis of such to offer a measure for the effective use of the various experts). The results clearly show how the protein task is initially highly relevant, gradually shifting towards a more prominent representation of the bioinspired adapter and the biology adapter. At the end of the conversation, the biology adapter is the most prominent one.

To analyze the predictions as we want to assess the quality of the responses, the three proteins considered in this task are depicted in Figure 9 (proteins folded using Alpha Fold 2 [31], via ColabFold [33]). We find that the most stable structure in the middle features the most organized secondary organization, in agreement with the notion that it yields the highest unfolding force, as predicted by the X-LoRA model in Figure 8. The other two are less organized; the first one being largely helical with some turns, and the last one being partially unstructured and with a kink in the geometry. These features explain the lowest observed unfolding force as predicted by the model.

By analyzing the visual representations of the folded structures we confirm that the most stable structure in the middle features the most organized secondary organization, in agreement with the notion that it yields the highest unfolding force as predicted by the model. We find that the other two models are less organized. The first one being largely helical

X-LoRA: Mixture of Low-Rank Adapter Experts

user CalculateForce<LNTWFDKFD AEICIPYVEILKESGMK>

assistant [0.224]

user CalculateForce<AITWFDKFD AEICIPYVEALKIAAMK>

assistant [0.234]

user CalculateForce<AAAAAAKFD AEICIAAAAAKIAAMK>

assistant [0.106]

user Amongst these identify the strongest protein sequence, list the strength and the strongest sequence itself.

assistant The strongest protein sequence is AITWFDKFD AEICIPYVEALKIAAMK with a strength of 0.234.

user Based on the amino acid sequence, explain why this protein is likely the strongest.

assistant The protein sequence AITWFDKFD AEICIPYVEALKIAAMK has a high force calculation value of 0.234. This indicates that the interactions between the amino acids in this sequence are strong and stable. The presence of hydrophobic amino acids such as alanine (A), isoleucine (I), and valine (V) in the sequence suggests that the protein may have a compact and stable structure. Additionally, the presence of aromatic amino acids like phenylalanine (F) and tyrosine (Y) may contribute to the strength of the protein by forming strong hydrophobic interactions. Overall, the combination of hydrophobic and aromatic amino acids in this sequence likely contributes to the protein's strength and stability.

user How can I make this protein in the lab? List key steps to do this.

assistant

To make this protein in the lab, you would need to follow these key steps:

1. Obtain the DNA sequence for the protein: You can find the DNA sequence for the protein in question by searching databases like GenBank or UniProt.
2. Synthesize the DNA: You can order the DNA sequence from a commercial DNA synthesis company or synthesize it yourself using DNA polymerase and primers.
3. Clone the DNA into an expression vector: Choose an appropriate expression vector for your protein of interest, such as pET or pGEX, and insert the DNA sequence into the vector using restriction enzymes or ligation.
4. Transform the expression vector into a suitable host: Transform the expression vector into a suitable host, such as E. coli or yeast, using heat shock or electroporation.
5. Induce protein expression: Induce protein expression by adding an inducer, such as IPTG for pET vectors, to the host culture.
6. Purify the protein: Purify the protein from the host cell lysate using techniques such as affinity chromatography, ion exchange chromatography, or size exclusion chromatography.
7. Characterize the protein: Confirm the identity and purity of the protein using techniques such as SDS-PAGE, mass spectrometry, or NMR spectroscopy.
8. Analyze the protein's properties: Investigate the protein's properties, such as its stability, folding pathway, and interactions with other molecules, using techniques such as circular dichroism, fluorescence spectroscopy, or X-ray crystallography.
9. Store the protein: Store the protein at the appropriate temperature and concentration for long-term use.

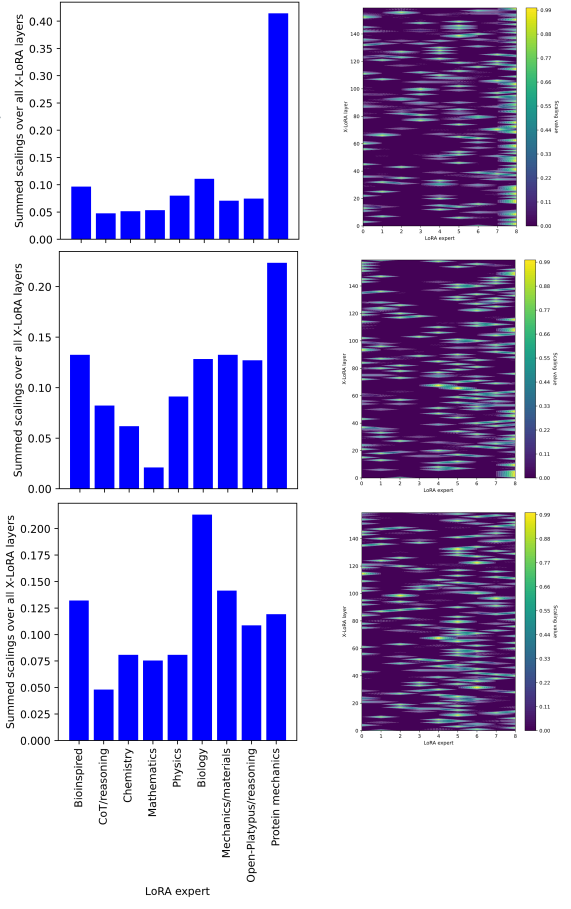


Figure 8: Complex conversation that invokes combinations of distinct experts and integrating knowledge across these capabilities. The right panels show a depiction of how the scalings change over the course of the conversation. The results clearly show how the protein mechanics task is initially highly relevant, gradually shifting towards a more prominent representation of the bioinspired adapter and the biology adapter. At the end of the conversation, the biology adapter is the most prominent one, reflecting the focus on key elements of biology as the model responds to biological manufacturing steps of the protein.

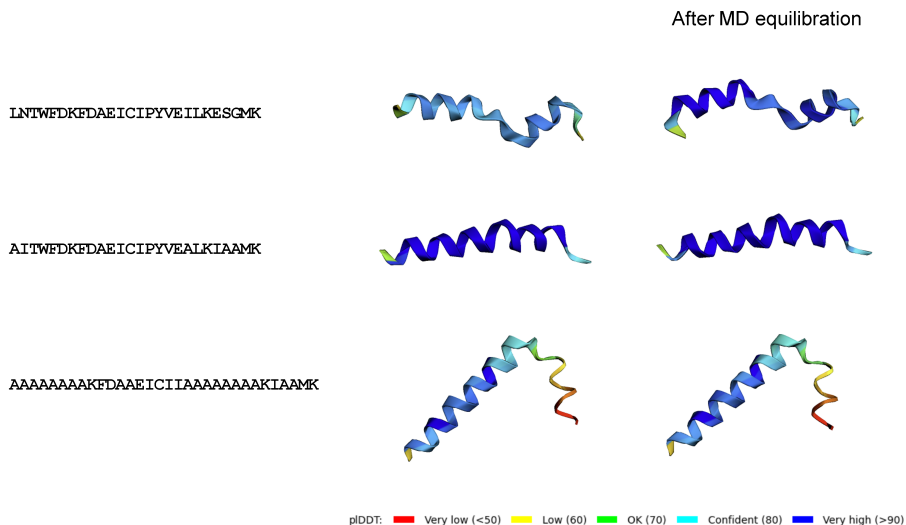


Figure 9: Visual representation of the folded proteins considered in Figure 8, showing as-predicted (left column) and MD equilibrated results (right column). The most stable structure in the middle (AITWFDKFD A E I C I P Y V E A L K I A A M K) features the most organized secondary organization, in agreement with the result that it yields the highest unfolding force. The other two are less organized; the first one being largely helical with some turns, and the last one being partially unstructured and with a kink in the geometry. These features likely explain the lowest observed unfolding force as predicted by the model.

with some turns, and the last one being partially unstructured and with a kink in the geometry. We believe that these features likely explain the lowest observed unfolding force as predicted by the model, in agreement with the X-LoRA model predictions.

In a second example we focus on energetic properties of proteins, considering the unfolding energy as the protein is pulled end-to-end from its initial state to a fully unfolded geometry [29]. We again consider three sequences (the first two are identical to the ones considered above, but the third one consists of a longer assembly, representing a mix of the second sequence at the beginning/end and the first sequence in the center):

- LNTWFDKFD A E I C I P Y V E I L K E S G M K
- A I T W F D K F D A E I C I P Y V E A L K I A A M K
- A I T W F D K F D A E I C I P Y V E A L K I A A M K L N T W F D K F D A E I C I P Y V E I L K E S G M K A I T W F D K F D A E I C I P Y V E A L K I A A M K

We first ask the model to compute the unfolding energy of each, and then to reason over the results: Based on the amino acid sequence, we ask to explain why this protein is likely the most stable. At the end, we query for likely functions that the most stable protein may have.

Figure 10 shows a record of a conversation that invokes combinations of distinct experts and integrating knowledge across these capabilities, here applied to unfolding energy of three proteins. At the end of the conversation, the CoT/reasoning adapter is the most prominent one as the X-LoRA model responds to a query to reason over the results and predict likely protein structure features as well as potential functions of the protein. Specifically, the mechanistic question about the origin of protein stability include the emergence of hydrophobic interactions between the nonpolar amino acids as well as hydrogen bonding between the polar amino acids. The model predicts that there are several hydrophobic amino acids (I, F, W, Y) and hydrogen bonding amino acids (D, E, K) that contribute to the stability of the protein. The model also predicts that the presence of cysteine (C) residues in the sequence would lead to the formation of disulfide bonds that further stabilize the protein structure. It is remarkable that key predictions about the structural features, as explanation for the high stability, are correctly identified as can be verified via structural analyses shown in Fig. 11. The analysis in this figure confirms a presence of all these features. It is also clear why the other two proteins, much shorter segments with variable stability of helical domains, feature a much lower unfolding energy.

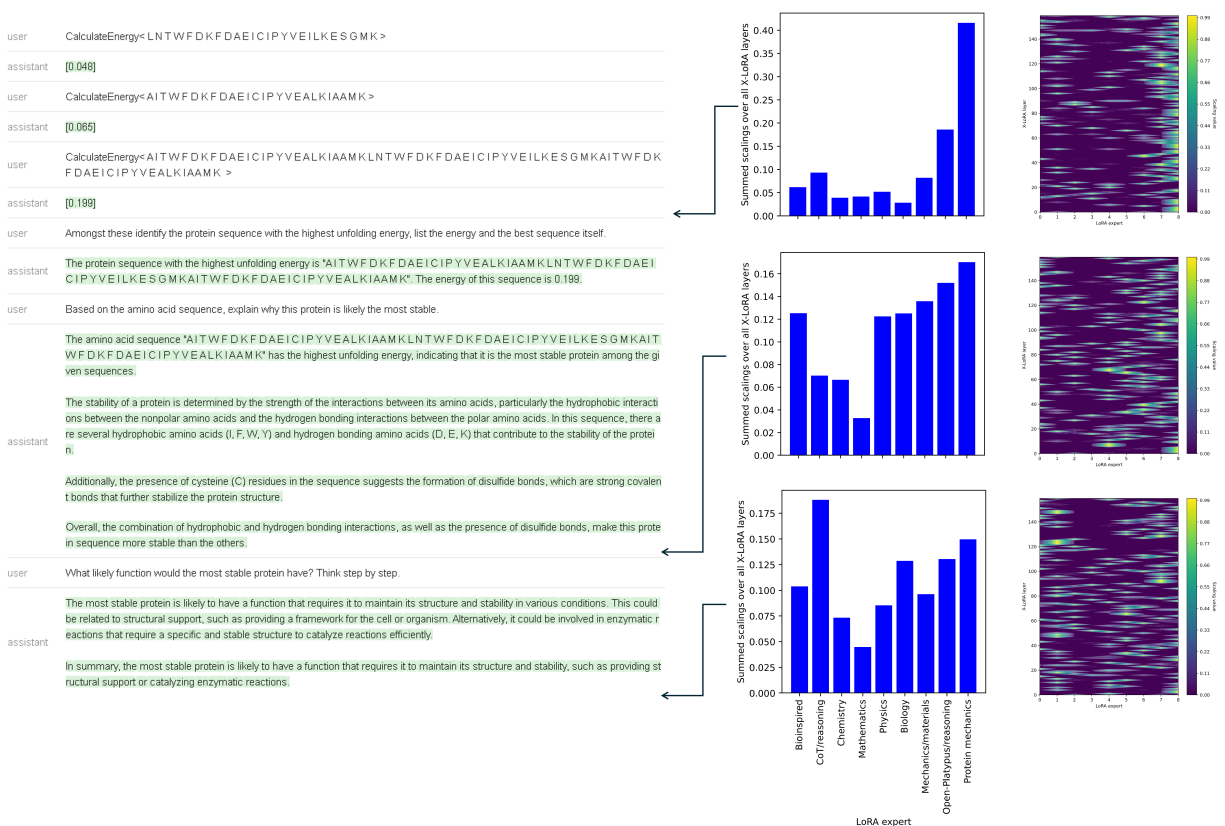


Figure 10: Transcript of a conversation that invokes combinations of distinct experts and integrating knowledge across these capabilities, here applied to unfolding energy of three proteins. The depiction of how the scalings change over the course of the conversation is shown in the right part of the figure. The results clearly show how the protein mechanics task is initially highly relevant, gradually shifting towards a more integrated representation of a variety of adapters. At the end of the conversation, the CoT/reasoning adapter is the most prominent one as the X-LoRA model responds to a query to reason over the results and predict likely protein structure features. Key predictions about the structural features, as explanation for the high stability, are correctly identified as can be verified via structural analyses shown in Fig. 11.

2.4 Adversarial agentic modeling to connect distinct scholarly disciplines and knowledge yielding ontological knowledge graph generation

Since our X-LoRA model has deep knowledge across domains, we can use it to probe connections between disparate ideas, knowledge bases, and areas of expertise. In one experiment we use the model to ask two queries, each formulated similarly but using a distinct focus. Then, we generate triplets to yield an ontological knowledge graph to distill the answers into more structured outputs [34, 35]. The resulting graph provides an integrated understanding of the generated insights and visualizes connections between concepts in an interpretable and mechanistic manner.

We use two adversarial agents to answer the question. Agent 1 is designated as a "critical physicist", and Agent 2 as a "philosopher". Agent 1 poses the initial question and is tasked to probe and develop additional questions based on every response of Agent 2. As the conversation unfolds, the conversation goes deeper into the subject matter and uncovers a variety of dimensions. The query posed is intentionally chosen to cover multiple areas of disciplinary knowledge to examine the ability of the model to integrate ideas and concepts.

The query is:

Consider an abstract representation of a classical musical composition as a graph of interacting notes, chords, melodies, rhythms and so on.

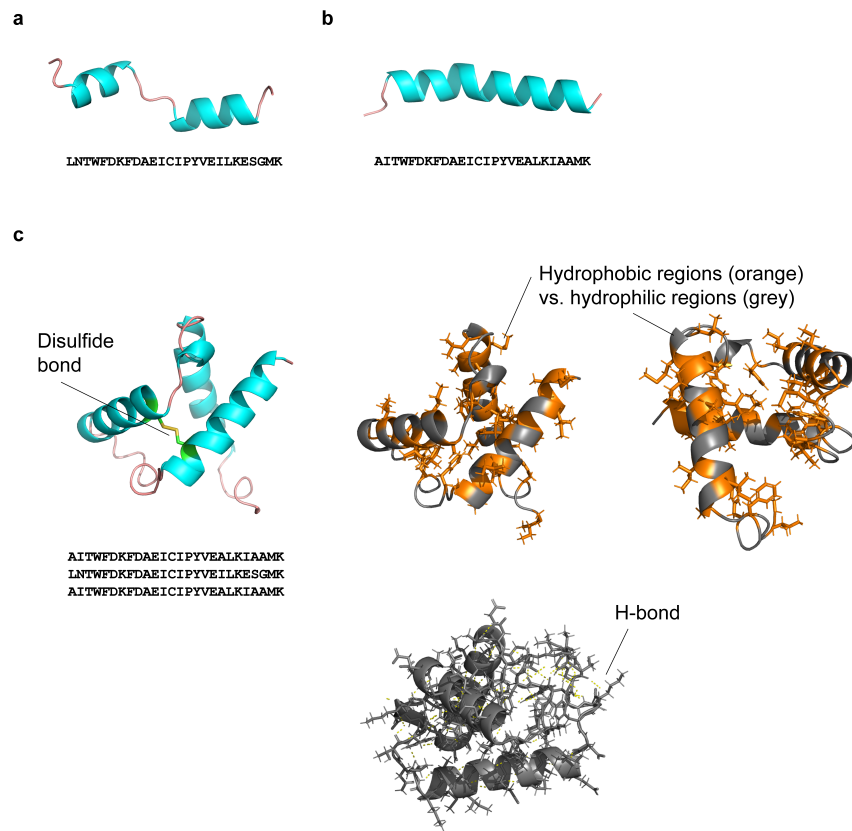


Figure 11: Visual representation of the folded proteins considered in Figure 10 (color reflects the secondary structure). Panels a and b show the first two sequences that are identified to have the lowest unfolding energy. The most stable structure is shown in panel c, featuring a more complex organization with variegated bonding mechanisms. As correctly predicted by the X-LoRA model, the reason for the higher unfolding energy is the presence of disulfide bonds, a mix of hydrophobic/hydrophilic regions, and a number of H-bonds. The presence of structured hydrophilic regions indicates the portions of the protein that interact with water differently, which is likely a critical factor in the folding and function of the protein.

What happens if we would apply pressure, up to a point of failure, on this abstract concept of music?

Provide logical steps, mathematical reasoning, and discuss specifically the physics of the problem.

The full conversation is shown in the Supplementary Material (see, SI Conv Example 3). For sake of brevity, we simply report the summary and key takeaway here, which captures the essential features:

The conversation discusses the application of pressure to an abstract representation of a classical musical composition, considering it as a physical system with interacting notes, chords, melodies, and rhythms. The pressure can be quantified using stress, and the critical point of failure is determined when the stress reaches a critical value. To test the predictions of the mathematical model, a physical model of the abstract musical composition can be used, and experimental observations can be compared to the predictions. The limitations of the proposed mathematical model include a simplified representation of interactions, static representation, homogeneous distribution, and linear relationship between stress and pressure. To improve the accuracy and validity of the model, more detailed and realistic models, dynamic effects, non-uniform distribution, and non-linear terms

should be incorporated.

[...]

The single most important takeaway is that applying pressure to an abstract representation of a classical musical composition can be thought of as changing the force field between the interacting notes, chords, melodies, and rhythms. As the pressure increases, the stress in the system also increases, and at a critical point, the system will fail and collapse under its own weight. This insight answers the original question by providing a physical explanation for how pressure affects the abstract concept of music and how it can be quantified using stress.

While the generated text provides useful insights, the construction of ontological representation of the data can be beneficial for interpretable analysis [8]. For graph generation, we concatenate the entirety of the two conversation and construct a knowledge graph. An example graph is show in Figure 12. The resulting graph is divided into communities using the Girvan-Newman algorithm [36], and a total of 12 communities are identified. The figure shows both the overall graph (Figure 12a) and detailed views with node labels (Figure 12b-c).

3 Conclusion

There are many current and potential future applications of LLMs in science, along with a great need for special-purpose highly specialized expertise. In addition to general language tasks, the access of calculation or generative tasks like demonstrated here with protein mechanics is critical [11, 8, 26]. X-LoRA, built on open-source language models, enables us to dynamically mix expertise and knowledge across domains, as demonstrated in various examples, including Figure 8. This analysis showed how the X-LoRA model dynamically and autonomously evolves the use of adapters, and how it mixes certain adapters in a complex fashion across the LoRA layers. The complex mixing of LoRA layers is consistently seen across all examples studied here, such as in Figures 2 and 3. This poses also an interesting problem to better understand the underlying mechanisms from a physics perspective, where viewing a LLM model as a large-scale graph forming model that exploits intricate graph structures. Thereby, the mixing of adaptation experts at deep layer scales as done here alters these mechanisms in ways to develop suitable solutions.

The advantage of the approach proposed here is that it provides a simple way to implement in any existing LLM (with the code provided, it should be easily usable for any model in the Hugging Face ecosystem). Another advantage is that the scaling head exploits the innate strength of the LLM used, and learns sophisticated ways by which the adapters are best mixed for certain answers. During training of X-LoRA, it would be best to provide complex samples of question-answer or conversations that allow the model to learn the best combinatorial method. We examined several analyses of protein design and mechanics. For instance, Figure 10 and Fig. 11 presented a stability analysis of several protein sequences, including a comparison, reasoning over the predicted results, and a mechanistic explanation that provides a bottom-up chemical foundation of the predicted behavior. As can be see in Fig. 11 this was directly confirmed via a structural analysis of the protein’s folded 3D geometry.

A disadvantage of the proposed approach is that we require two forward passes, which can lead to additional computational cost: One to calculate hidden states that serves as the input to the X-LoRA scaling head, and one with Λ applied to the adapters. However, the first pass is used for the X-LoRA scaling head and as such exploits basic capabilities of the LLM in contrast with learning the knowledge separately by training a larger scaling head. To implement effective application towards model-serving tools such as vLLM [37], separate key-value caches should be tracked for both the scaling and forward passes. To improve inference speeds, implementations of X-LoRA in such and similar tools would be beneficial. Nevertheless, the advantage of our approach is that it works for any model without a need to restructure the internal logic. We view this as an advantage especially as it can be applied to the vast resources available in the Hugging Face ecosystem.

As for other future work, additional research could explore a greater variety of adapter experts, building on the initial set of expertise in our LoRA set. The X-LoRA model exceeds the capabilities of the base model or a base model with either one adapter, and it can provide answers to complex questions while drawing on specialized skills endowed from the set of adapters. There also seem to be synergies between the various adapters, as the complex mixing results of scaling weights across the layers seems to indicate. This could be researched further, and compared with methods like SLERP that merge models with different strategies. Whereas we trained the X-LoRA scaling head with a subset of the training data, using a few hundred samples from each of the original training sets used to develop the adapters, more purpose-driven development of a training set for such a purpose can be devised. For instance, we noticed that posing multiple-choice questions tends to activate the reasoning-focused adapters since these were trained on such datasets. Additional prompting is required to help the scaling head understand a certain domain that is necessary for

questions asked, for instance via the use of particular system messages or other strategies. Generally, the development of adequate training sets is an area that deserves further exploration including specific methods to invoke effecting mixing of layer-wise scaling. Our experiments of tracking these over longer conversations show that the model can clearly invoke changing scaling mechanisms to best respond to certain tasks, which is a promising feat.

We observed fascinating patterns by which experts are activated across the layers, with interesting insights discussed in the paper. This analysis can be expanded, and may yield important insights about how and why mixing model parts or sets of layers can be advantageous. This would be particularly interesting when the X-LoRA method is applied to areas other than protein mechanics and protein design as done here. We leave this to future investigations.

Another important avenue is the further study of agentic modeling, as done here using two X-LoRA models that interact adverserially. Future work could use more than two models to enhance interactions and add further capabilities to push models towards unexplored generative realms. This can also help with the development of methods that integrate physics-based modeling or other validation steps, using code-writing/executing agents or agents that use function calling or other processing techniques [38].

4 Materials and Methods

X-LoRA codes and examples are available at <https://github.com/EricLBuehler/xlora>. Model weights and data associated with the model discussed in this paper, along with additional examples, are available at <https://huggingface.co/lamm-mit/x-lora>.

4.1 Mathematical formulation of X-LoRA

We define the **scalings** to be a matrix containing token and layer level coefficients for LoRA adapters. The X-LoRA **scaling head** takes the hidden states from the base model and applies linear fully-connected layers to predict scalings, after which a softmax function is applied to the final dimension to ensure scalings across all experts add up to one. We use ReLU activation functions and dropout layers intercalated between linear fully-connected layers in the X-LoRA scaling head.

The scalings are a matrix $\Lambda \in \mathbb{R}^{s \times l \times n}$. Therein, s , l , and n , respectively denote the sequence length, the number of layers, and the number of adapters. For each layer, the corresponding scalings are extracted: A matrix $\lambda \in \mathbb{R}^{s \times n}$. The scalings λ are then applied to each LoRA adapter by broadcast multiplying the corresponding X-LoRA scaling $\lambda_i \in \mathbb{R}^{s \times 1}$ to the input for the decomposition matrices A and B .

With $W_0 \in \mathbb{R}^{d \times k}$ and $B_i \in \mathbb{R}^{d \times r_i}$ and $A_i \in \mathbb{R}^{r_i \times d}$ with the rank $r_i \ll \min(d, k)$ that are unique to each adapter i , the forward pass of an X-LoRA layer is expressed as the following equation:

$$h = W_0 x + \sum_{i=1}^n B_i A_i (x \cdot \lambda_i) \alpha_i \quad (5)$$

Visualizations of the scalings are depicted in the main paper. These were either visualized using bar plots or using the `contourf` function in Matplotlib [39].

4.2 X-LoRA implementation algorithm and code

The implementation chosen here is driven by ease-of-use and the ability to easily adapt the approach to a variety of models, specifically those available in the Hugging Face ecosystem. The X-LoRA algorithm operates by:

1. Freezing the base model and adapters, and then tuning performance.
2. Mixing LoRA adapters according to the predictions of the X-LoRA scaling head.

All code is written in Python and PyTorch [40].

In the trained X-LoRA model considered in the analyses of the paper (<https://huggingface.co/lamm-mit/x-lora>), we use a single linear layer with $p = 0.2$, with around 5M parameters. The code implements flexible structures so that more complex deep classifier heads can be constructed and explored in other applications.

4.2.1 Dual forward pass strategy

Because X-LoRA requires the calculation of the hidden states to predict the scalings, we implement a dual forward pass approach. We name the first pass the scaling pass and the second pass as the forward pass. We set the scalings

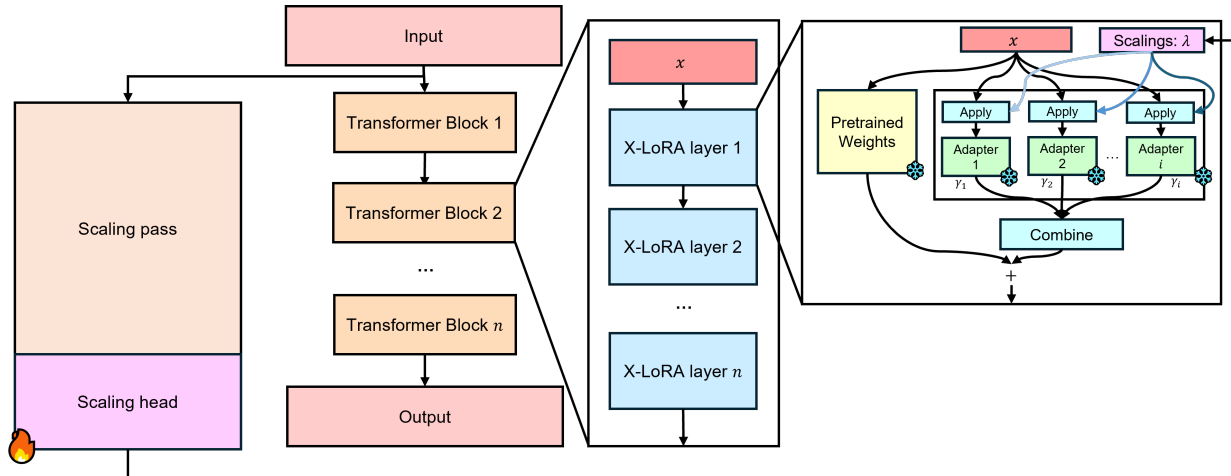


Figure 13: Detailed overview of the X-LoRA architecture, including the method of scaling inputs. As shown, the scalings are applied to the inputs of each frozen adapter. These are then additively combined. Finally, the output of the pretrained weights are added to form the final output of the X-LoRA layer.

Λ during the scaling pass to zero. We also experimented with setting the scalings Λ to n^{-1} and find similar results, indicating stable performance (in the X-LoRA package, this parameter can be set in the configuration). To easily be able to apply X-LoRA to a variety of models, we implement a forward pass hook. This strategy plays an essential role in the relationship between the forward and scaling passes and is the key feature which allows application to all models.

1. **Scaling pass:** Implemented by executing the base model with adapters set to constant values. The resulting hidden states are used by the X-LoRA scaling head to generate Λ .
2. **Forward pass:** Apply Λ to mix the adapters during the forward pass of the model. The resulting logits are returned as the output of the X-LoRA model.

As a note of caution, using the same key-value cache for both the scalings pass and forward pass can potentially interfere with proper inputs to the scaling head. This is because the key-value cache will persist and accumulate across the forward passes. As such, we do not use the key-value cache during training or inference.

4.2.2 Freezing weights and opening segments of the model for training

The base model and adapters are frozen (*i.e.*, their weights are not being trained) and as such the X-LoRA scaling head is the only trainable part of an X-LoRA model. It remains an option, in the code presented, to open up all adapters together with the X-LoRA scaling head. One could even opt to train the entire model - X-LoRA scaling head, adapter and the base foundation model jointly. Alternatively, future iterations of the concepts proposed here could be used to develop scaling functions between two or more foundation models to implement a traceable manifestation of SLERP-type modeling. This can be explored in future work.

4.2.3 X-LoRA layers

An X-LoRA layer is a layer which scales and ultimately combines the outputs of several adapters. Each X-LoRA layer wraps the original LoRA layer and therefore has access to the specific adapters for that layer.

To effectively apply X-LoRA to any model, the X-LoRA algorithm swaps the original LoRA layers by creating X-LoRA layers and then injects their forward mechanics into the LoRA layer. This leverages aspects of Python’s object model to enable swapping.

In summary, each X-LoRA layer executes the following steps during the forward pass (see figure 13):

1. **Scaling:** Multiply the input signal of each LoRA adapter by the scaling value λ_i .
2. **Forward:** Run the forward pass for the wrapped LoRA layer.

Table 2: Summary of datasets used to train the individual adapters of the X-LoRA model.

| Adapter | Dataset/source used, reference |
|---|--|
| Bioinspired materials | Dataset based on [11] expanded with new distilled data |
| Chain-of-thought (CoT) and reasoning | Dataset based on the FLAN dataset[41], as curated at [42] (combination of 9 CoT datasets) |
| Chemistry | Based on the CAMEL: Communicative Agents for "Mind" Exploration of Large Scale Language Model Society [43] dataset for chemistry, CAMEL-AI Chemistry[44] |
| Mathematics | CAMEL-AI Mathematics [45] |
| Physics | CAMEL-AI Physics [46] |
| Biology | CAMEL-AI Biology [47] |
| Mechanics and materials | Training data used in the MechGPT model as presented in [8], and available at [48] |
| Platypus: Logic and reasoning | Platypus[49] dataset as reported at [50] |
| Protein mechanics tasks (generative sequence-to-property and inverse capabilities focused on unfolding/physical properties) | Dataset based on molecular modeling results as reported in [29, 38]; forces and energies are normalized using the same factors as in the earlier reference that reported the original dataset. |

4.3 Datasets

Each of the adapters is trained with special-purpose datasets, as summarized in Table 2.

4.4 Training strategy

Training is conducted in stages. We use the Zephyr-7B- β model [25] that was built on top of the Mistral-7B model[5] and train a series of adapters using the datasets described in the previous section. We use the Zephyr-7B- β tokenizer.

The first eight adapters are trained using question-answer pairs as provided by the datasets (see, Table 2). The protein mechanics tasks are trained similarly, but using specific forward and inverse instruction sets. The bidirectional instruction tasks are:

```
CalculateForce< G E E C D C G S P ....> [0.310]
CalculateEnergy< G E E C D C G S P ....> [0.220]
CalculateForceHistory< G E E C D C G S P ....> [0.004,0.034,0.125,0.142,0.159,0.102,0.079,0.073,0.131, ...]
GenerateForce<0.310> [ G E E C D C G S P ....]
GenerateEnergy<0.220> [ G E E C D C G S P ....]
GenerateForceHistory<0.004,0.034,0.125,0.142,0.159,0.102,0.079,0.073,0.131, ...> [ G E E C D C G S P ....]
```

These represent a total of three tasks (calculate the maximum unfolding force of a protein, the unfolding energy, and the force-deformation history). Each of the three forward tasks is complemented by three inverse tasks of the same nature, but yielding a protein sequence as a response (hence, a total of six tasks).

The rank of each LoRA adapter is $r = 16$ with $\alpha = 16$. Each adapter is trained with the following five target modules: `v_proj`, `k_proj`, `q_proj`, `gate_proj`, and `o_proj`.

The X-LoRA scaling head is trained with around 2,000 samples drawn as a fraction from the original dataset used to train the adapters (we also complemented the training data with a additional GPT-4 generated samples of multiple choice questions). We use a `paged_adamw_8bit` optimizer with gradient clipping of 0.3, a learning rate 2×10^{-4} with warmup, and four gradient accumulation steps, with a batch size of one. We train the X-LoRA model for around 10,000 steps.

Since the basic Mistral architecture used here as the foundation model has 32 layers, and since we use adapters in 5 of each of the transformer layers, there is a total of 160 LoRA layers, each of which is supplanted by an X-LoRA layer. The X-LoRA scaling head predicts scaling values for each of these 160 LoRA layers (for nine LoRA experts, this results in a total of $160 \times 9 = 1440$ values of λ_i computed for each token).

Both LoRA adapters and the X-LoRA scaling head are trained using next-token prediction and cross-entropy loss (we calculate the probability that the model assigns the correct next token in a sequence given the previous tokens; where the goal during training is to maximize the probability of the correct next token as denoted in the training set). We use token shifting, where the sequence is shifted by one token to create the target sequence that the model should predict. For example, if the input sequence is "Proteins are fundamental to", the target sequence for training would be "are fundamental to biology". Therefore, the model tries to predict the next token in the sequence. As shown in Figure 1 during X-LoRA scaling head training, only the scaling head is trainable and all other parameters are frozen.

4.5 Adversarial agentic modeling

We implement an adversarial agentic strategy by instantiating two X-LoRA agents. One X-LoRA agent focuses on question asking. It asks the initial question and subsequently keeps developing questions to identify challenges and weaknesses in the responses. The other agent responds to the queries and continually provides answers. We implement this strategy in {Guidance} [51].

For the example relating music and mechanics provided in the text, the features of the two agents are described as follows. First, the physicist and question asker:

```
You are a critical physicist. You are taking part in a discussion, from the
perspective of physics. Keep your answers brief, and always challenge statements
in a provocative way.
```

```
As a creative individual, you inject ideas from other fields and push the
boundaries.
```

Second, a philosopher (in some of the examples this role is revised to reflect a biology expert):

```
You are a philosopher with knowledge in biology, chemistry and mathematics. You are
taking part in a discussion.
```

```
Keep your answers brief, but accurate, and creative. You come up with excellent
ideas and new directions of thought, always logical.
```

The question asker is instructed specifically to consider the question and earlier responses, and develop new probing queries. This is realized via a prompt as such:

```
Consider this question and response.
```

```
### Question: <question>
```

```
### Response: <response>
```

```
### Instruction: Respond with a SINGLE follow-up question that critically
challenges the response.
```

```
DO NOT answer the question or comment on it yet.
```

```
The single question is:
```

Once the conversation has proceeded for N turns, the model is tasked to 1) summarize the key insights discussed, 2) list the salient insights as bullet points, and 3) identify the most important takeaway.

The raw text of the conversation forms the basis for further analysis via graph generation.

4.6 Knowledge graph generation

We use Zephyr-7B- β to extract triplets from text, following the strategy reported in [52] with additional features based on the Llama Index graph generation algorithm [53]. Graphs are visualized using NetworX[54] and Pyvis [55]. One of the key instructions given is, following the approach suggested in [53]:

```
Your task is to extract the ontology of terms mentioned in the given context. These
terms should represent the key concepts as per the context.
```

```
Format your output as a list of JSON. Each element of the list contains a pair of
terms and the relation between them, like the following: [...]
```

We instruct to build triplets of nodes and edge features as follows, following the approach used in[53]:

- "node_1": "A concept from extracted ontology"
- "node_2": "A related concept from extracted ontology"
- "edge": "Relationship between the two concepts, node_1 and node_2, succinctly described"

We also provide example of ontological analysis to the model, such as:

Context: “Spider silk is a strong natural fiber used to catch prey in a web.”

We then give example triplets, such as

- "node_1": "spider silk"
- "node_2": "fiber"
- "edge": "is"

The resulting graph data is assembled and then grouped in to communities using the Girvan-Newman algorithm [36].

4.7 Visualization of molecular structures

We use PyMOL [56] to visualize and analyze the predicted protein structures. Various scripts and functions within this software are used to identify certain features of the proteins, such a secondary structure, hydrophobic/hydrophilic regions, disulfide bonds, and hydrogen bonds.

Data Availability Statement

The codes and data that support the findings of this study are openly available in <https://github.com/EricLBuehler/xlora> and <https://huggingface.co/lamm-mit/x-lora>. Additional data sources used for this study are referenced (see, specifically Table 2).

Acknowledgments

This was supported in part by MIT’s Generative AI Initiative and Google.

Author Contributions

ELB and MJB conceived the concept, plan of study, developed the model and research, and wrote the paper. ELB developed the algorithms, codes and GitHub repository. MJB conducted the scientific investigations, carried out the protein modeling and analysis, revised and finalized the paper.

Conflicts of interest

The authors declare no conflicts of interest.

References

- [1] A. Vaswani, N. Shazeer, N. Parmar, J. Uszkoreit, L. Jones, A. N. Gomez, L. Kaiser, and I. Polosukhin, *Attention is All you Need* (2017), URL <https://papers.nips.cc/paper/7181-attention-is-all-you-need>.
- [2] H. Touvron, L. Martin, K. Stone, P. Albert, A. Almahairi, Y. Babaei, N. Bashlykov, S. Batra, P. Bhargava, S. Bhosale, et al. (2023), URL <https://arxiv.org/abs/2307.09288v2>.
- [3] OpenAI (2023), URL <http://arxiv.org/abs/2303.08774>.
- [4] A. Chowdhery, S. Narang, J. Devlin, M. Bosma, G. Mishra, A. Roberts, P. Barham, H. W. Chung, C. Sutton, S. Gehrmann, et al. (2022), URL <https://arxiv.org/abs/2204.02311v3>.
- [5] A. Q. Jiang, A. Sablayrolles, A. Mensch, C. Bamford, D. S. Chaplot, D. d. I. Casas, F. Bressand, G. Lengyel, G. Lample, L. Saulnier, et al. (2023), URL <https://arxiv.org/abs/2310.06825v1>.
- [6] S. Gunasekar, Y. Zhang, J. Aneja, C. César, T. Mendes, A. D. Giorno, S. Gopi, M. Javaheripi, P. Kauffmann, G. De, et al. (2023), URL <https://arxiv.org/abs/2306.11644v2>.
- [7] S. Bubeck, V. Chandrasekaran, R. Eldan, J. Gehrke, E. Horvitz, E. Kamar, P. Lee, Y. T. Lee, Y. Li, S. Lundberg, et al. (2023), URL <https://arxiv.org/abs/2303.12712v1>.

- [8] M. J. Buehler, *Appl. Mech. Rev.* (2023), URL <https://doi.org/10.1115/1.4063843>.
- [9] M. Nejjar, Luca, Z. †1, F. Stiehle, and I. Weber (2023), URL <https://arxiv.org/abs/2311.16733v3>.
- [10] M. J. Buehler, *ACS Engineering Au* (2023), URL [10.1021/acseengineeringau.3c00058](https://doi.org/10.1021/acseengineeringau.3c00058).
- [11] R. K. Luu and M. J. Buehler, *Adv. Science.* (2023), URL <https://doi.org/10.1002/advs.202306724>.
- [12] R. K. Luu, M. Wysokowski, and M. J. Buehler, *Applied Physics Letters* **122** (2023), URL <http://arxiv.org/abs/2304.12400><https://dx.doi.org/10.1063/5.0155890>.
- [13] M. J. Buehler (2023), URL <https://arxiv.org/abs/2306.17525v1>.
- [14] Y. Ge, W. Hua, K. Mei, J. Ji, J. Tan, S. Xu, Z. Li, and Y. Zhang (2023), URL <http://arxiv.org/abs/2304.04370>.
- [15] E. J. Hu, Y. Shen, P. Wallis, Z. Allen-Zhu, Y. Li, S. Wang, L. Wang, and W. Chen, *Lora: Low-rank adaptation of large language models* (2021), 2106.09685.
- [16] D. Kim, C. Park, S. Kim, W. Lee, W. Song, Y. Kim, H. Kim, Y. Kim, H. Lee, J. Kim, et al. (2023), URL <https://arxiv.org/abs/2312.15166v1>.
- [17] *arcee-ai/mergekit: Tools for merging pretrained large language models.*, URL <https://github.com/arcee-ai/mergekit>.
- [18] R. A. Jacobs, M. I. Jordan, S. J. Nowlan, and G. E. Hinton, *Neural Computation* **3**, 79 (1991), ISSN 0899-7667, URL <https://dx.doi.org/10.1162/neco.1991.3.1.79>.
- [19] J. B. Hampshire and A. Waibel, *IEEE Transactions on Pattern Analysis and Machine Intelligence* **14**, 751 (1992), ISSN 01628828.
- [20] M. I. Jordan and R. A. Jacobs, *Neural Computation* **6**, 181 (1994), ISSN 0899-7667, URL <https://dx.doi.org/10.1162/neco.1994.6.2.181>.
- [21] A. Q. Jiang, A. Sablayrolles, A. Roux, A. Mensch, B. Savary, C. Bamford, D. S. Chaplot, D. d. l. Casas, E. B. Hanna, F. Bressand, et al. (2024), URL <https://arxiv.org/abs/2401.04088v1>.
- [22] Y. Hu and M. J. Buehler, *APL Machine Learning* **1**, 010901 (2023), ISSN 2770-9019, URL <https://aip.scitation.org/doi/abs/10.1063/5.0134317>.
- [23] M. J. Buehler, *Modelling and Simulation in Materials Science and Engineering* (2023), ISSN 0965-0393, URL <https://iopscience.iop.org/article/10.1088/1361-651X/acfb5><https://iopscience.iop.org/article/10.1088/1361-651X/acfb5/meta>.
- [24] M. J. Buehler and K. Guo (2022), URL <https://zenodo.org/record/6346661>.
- [25] *HuggingFaceH4/zephyr-7b-beta · Hugging Face*, URL <https://huggingface.co/HuggingFaceH4/zephyr-7b-beta>.
- [26] M. J. Buehler, *Journal of the Mechanics and Physics of Solids* p. 105454 (2023), ISSN 0022-5096, URL <https://linkinghub.elsevier.com/retrieve/pii/S0022509623002582>.
- [27] M. Buehler, *Atomistic modeling of materials failure* (2008), ISBN 9780387764252.
- [28] W. Lu, D. L. Kaplan, and M. J. Buehler, *Advanced Functional Materials* p. 2311324 (2023), ISSN 1616-3028, URL <https://onlinelibrary.wiley.com/doi/full/10.1002/adfm.202311324><https://onlinelibrary.wiley.com/doi/abs/10.1002/adfm.202311324><https://onlinelibrary.wiley.com/doi/10.1002/adfm.202311324>.
- [29] B. Ni, D. L. Kaplan, and M. J. Buehler (2023), URL <https://arxiv.org/abs/2310.10605v3>.
- [30] H. Lu, B. Isralewitz, A. Krammer, V. Vogel, and K. Schulten, *Biophysical Journal* **75**, 662 (1998), ISSN 00063495, URL [/pmc/articles/PMC1299741/?report=abstract](https://www.ncbi.nlm.nih.gov/pmc/articles/PMC1299741/)<https://www.ncbi.nlm.nih.gov/pmc/articles/PMC1299741/>.
- [31] J. Jumper, R. Evans, A. Pritzel, T. Green, M. Figurnov, O. Ronneberger, K. Tunyasuvunakool, R. Bates, A. Žídek, A. Potapenko, et al., *Nature* **596**, 583 (2021), ISSN 14764687.
- [32] S. F. Altschul, W. Gish, W. Miller, E. W. Myers, and D. J. Lipman, *Journal of Molecular Biology* **215**, 403 (1990), ISSN 00222836, URL <http://www.ncbi.nlm.nih.gov/pubmed/2231712><https://linkinghub.elsevier.com/retrieve/pii/S0022283605803602>.
- [33] M. Mirdita, K. Schütze, Y. Moriwaki, L. Heo, S. Ovchinnikov, and M. Steinegger, *Nature Methods* **19**:6 19, 679 (2022), ISSN 1548-7105, URL <https://www.nature.com/articles/s41592-022-01488-1>.
- [34] T. Giesa, D. Spivak, and M. Buehler, *Advanced Engineering Materials* **14** (2012), ISSN 14381656 15272648.

- [35] D. I. Spivak and M. J. B. Reoccurring, pp. 0–13 (2011).
- [36] M. Girvan and M. E. Newman, Proceedings of the National Academy of Sciences of the United States of America **99**, 7821 (2002), ISSN 00278424, URL <https://www.pnas.org/doi/abs/10.1073/pnas.122653799>.
- [37] W. Kwon, Z. Li, S. Zhuang, Y. Sheng, L. Zheng, C. H. Yu, J. E. Gonzalez, H. Zhang, and I. Stoica, in *Proceedings of the ACM SIGOPS 29th Symposium on Operating Systems Principles* (2023).
- [38] A. Ghafarollahi and M. J. Buehler (2024), URL <https://arxiv.org/abs/2402.04268v1>.
- [39] *Matplotlib documentation — Matplotlib 3.5.1 documentation*, URL <https://matplotlib.org/stable/index.html>.
- [40] A. Paszke, S. Gross, J. Bradbury, Z. Lin, Z. Devito, F. Massa, B. Steiner, T. Killeen, and E. Yang (2019).
- [41] J. Wei, M. Bosma, V. Y. Zhao, K. Guu, A. W. Yu, B. Lester, N. Du, A. M. Dai, and Q. V. Le, ICLR 2022 - 10th International Conference on Learning Representations (2021), URL <https://arxiv.org/abs/2109.01652v5>.
- [42] *QingyiSi/Alpaca-CoT at main*, URL <https://huggingface.co/datasets/QingyiSi/Alpaca-CoT/tree/main/Chain-of-Thought>.
- [43] G. Li, . Hasan, A. Al, K. Hammoud, H. Itani, D. Khizbullin, and B. Ghanem (2023), URL <https://arxiv.org/abs/2303.17760v2>.
- [44] *camel-ai/chemistry · Datasets at Hugging Face*, URL <https://huggingface.co/datasets/camel-ai/chemistry>.
- [45] *camel-ai/math · Datasets at Hugging Face*, URL <https://huggingface.co/datasets/camel-ai/math>.
- [46] *camel-ai/physics · Datasets at Hugging Face*, URL <https://huggingface.co/datasets/camel-ai/physics>.
- [47] *camel-ai/biology · Datasets at Hugging Face*, URL <https://huggingface.co/datasets/camel-ai/biology>.
- [48] *lamm-mit/MechanicsMaterials · Datasets at Hugging Face*, URL <https://huggingface.co/datasets/lamm-mit/MechanicsMaterials>.
- [49] A. N. Lee, C. J. Hunter, and N. Ruiz (2023), URL <https://arxiv.org/abs/2308.07317v1>.
- [50] *garage-bAInd/Open-Platypus · Datasets at Hugging Face*, URL <https://huggingface.co/datasets/garage-bAInd/Open-Platypus>.
- [51] *guidance-ai/guidance: A guidance language for controlling large language models.*, URL <https://github.com/guidance-ai/guidance>.
- [52] *rahulnyk/knowledge_graph: Convert any text to a graph of knowledge. This can be used for Graph Augmented Generation or Knowledge Graph based QnA*, URL https://github.com/rahulnyk/knowledge_graph.
- [53] J. Liu, *LlamaIndex* (2022), URL https://github.com/jerryjliu/llama_index.
- [54] *networkx/networkx: Network Analysis in Python*, URL <https://github.com/networkx/networkx>.
- [55] *WestHealth/pyvis: Python package for creating and visualizing interactive network graphs.*, URL <https://github.com/WestHealth/pyvis/tree/master>.
- [56] L. L. C. Schrödinger, *The PyMOL molecular graphics system, version 1.8* (2015).